Chem Soc Rev

Photoinduced electron transfer across molecular bridges. Electron- and hole-transfer superexchange pathways

Journal:	*Chemical Society Reviews*
Manuscript ID:	CS-TRV-12-2013-060463.R2
Article Type:	Tutorial Review
Date Submitted by the Author:	05-Feb-2014
Complete List of Authors:	Campagna, Sebastiano; University of Messina, Dipartimento di Scienze Chimiche Scandola, Franco; Universita' di Ferrara, Dipartimento di Scienze Chimiche e Farmaceutiche Natali, Mirco; Universita' di Ferrara, Dipartimento di Chimica

Journal Name

RSCPublishing

ARTICLE

Photoinduced electron transfer across molecular bridges. Electron- and hole-transfer superexchange pathways.

Cite this: DOI: 10.1039/xoxxoooooox

Received ooth January 2012,
Accepted ooth January 2012

DOI: 10.1039/xoxxoooooox

www.rsc.org/

Mirco Natali,[a] Sebastiano Campagna*[b] and Franco Scandola*[a]

Photoinduced electron transfer plays key roles in many areas of chemistry. Superexchange is an effective model to rationalize photoinduced electron transfer, particularly when molecular bridges between donor and acceptor subunits are present. In this tutorial review we discuss, within a superexchange framework, the complex role played by the bridge, with emphasis on differences between thermal and photoinduced electron transfer, oxidative and reductive photoinduced processes, charge separation and charge recombination. Modular bridges are also considered, with specific attention to the distance dipendence of donor-acceptor electronic coupling and electron transfer rate constants. The possibility of transition, depending on the bridge energetics, from coherent donor-acceptor electron transfer to incoherent charge injection and hopping through the bridge is also discussed. Finally, conceptual analogies between bridge effects in photoinduced electron transfer and optical intervalence transfer are outlined. Selected experimental examples, instrumental to illustration of the principles, are discussed.

1. Introduction

Electron Transfer (ET) can be definitely considered the single most important chemical reaction.[1] As an elementary chemical process, it is amenable to very detailed theoretical description[2a-d] and experimental investigation.[2e] In reality, it constitutes a key step in biological processes of enormous relevance to life[3,4] and in artificial systems of great technological impact.[5-7] Most of the recent fundamental advances in the understanding of this field have been obtained by studying ET processes taking place in systems where a donor (D) and an acceptor (A) molecular units are chemically connected by some kind of rigid bridge (B). In such donor-bridge-acceptor (D-B-A) systems, ET can be conveniently triggered by applying some kind of fast perturbation, typically, though not uniquely, light excitation (photoinduced electron transfer, PET). Being unimolecular in nature, such processes in D-B-A systems are free of the diffusional complications inherent to the analogous bimolecular processes of D and A, and are thus much more easily amenable to theoretical treatment. Also, having the donor and acceptor held at a fixed distance by a chemical bridge, ET studies on D-B-A systems can give important information on the dependence of ET processes on the donor-acceptor distance. In most cases, however, the bridge is not just operating as an inert spacer building block, but is found to play a distinct role in favoring charge transfer between donor and acceptor. Thus, a further point of interest in the study of D-B-A systems is the understanding of how the structure and chemical nature of the bridge influences ET. This is precisely where the main focus of this review lies. Though introduced here for simple D-B-A systems, the subject is of more general relevance, being crucial in several related fields of practical importance, such as ET in biological systems, charge transport in polymeric materials, signal transduction in opto-electronic devices.

In this tutorial review, we will first outline a general conceptual scheme, based on superexchange, to describe the role of the bridge in ET processes in D-B-A systems. While the literature on ET in D-B-A systems is extremely vast, and a number of excellent reviews[8] and monographs[1,9] are available, our aim here is to provide the reader approaching the subject with a reasonably simple but consistent general picture. The introductory part is then followed by a discussion of selected examples from the literature. The examples are chosen, aside from novelty or intrinsic interest, for their appropriateness to illustrate specific aspects of this multifaceted subject.

2. Electron transfer

From a quantum mechanical viewpoint, ET in a donor-bridge-acceptor system (eq 1), can be viewed as a

$$D\text{-}B\text{-}A \rightarrow D^{+}\text{-}B\text{-}A^{-} \quad (1)$$

radiationless transition between different, weakly interacting electronic states of the D-B-A supermolecule. Using a Fermi Golden Rule formalism (eq 2), the rate constant can be expressed as the product of an electronic, H_{ET}, and a nuclear term, *FCWD*.[10-13]

$$k_{el} = \frac{4\pi^2}{h}|H_{ET}|^2 FCWD \quad (2)$$

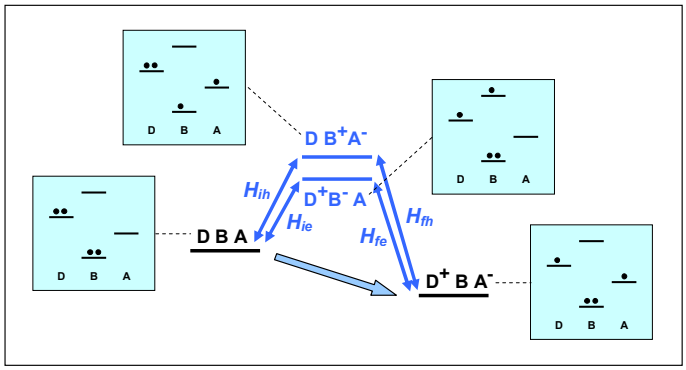

Fig. 1. Schematic representation of the superexchange interactions mediating ET in D-B-A molecular dyads. The various states (virtual states in blue) are sketched in terms of one-electron configurations in the associated boxes. Couplings are represented by double arrows connecting the states. For further details, see text.

The Franck-Condon weighted density of states, *FCWD*, is a thermally averaged overlap between the reactant and product vibrational wavefunctions. In a single-mode approximation, with quantum mode of frequency ν_i, this term is given by[12]

$$FCWD = \left(\frac{1}{4\pi\lambda_o k_B T}\right)^{\frac{1}{2}} \sum_m S^m \frac{e^{-S}}{m!} \exp\left[-\frac{(\Delta G^0 + \lambda_o + mh\nu_i)^2}{4\lambda_o k_B T}\right] \quad (3)$$

$$S = \frac{\lambda_i}{h\nu_i} \quad (4)$$

where the sum in eq 3 extends over m, the number of vibrational quanta in the product state, ΔG^0 is the free energy change, S is the Huang-Rhys factor (a dimensionless displacement parameter proportional, eq 4, to the inner-sphere reorganization energy λ_i, and λ_o is the classical outer-sphere (solvent) reorganization energy.[11d] The *FCWD* term, which in the high-temperature limit yields the classical expression of the Marcus theory[11d] for the free energy of activation (eq 5),

$$FCWD = \left(\frac{1}{4\pi\lambda k_B T}\right)^{\frac{1}{2}} \exp\left[-\frac{(\Delta G^0 + \lambda)^2}{4\lambda k_B T}\right] \quad (5)$$

accounts for the combined effects of the nuclear reorganization and driving force. In particular, it predicts "normal", activationless, or "inverted" kinetic regimes depending on whether $-\Delta G°$ is smaller than, equal to, or larger than $\lambda = (\lambda_i + \lambda_o)$. While the nuclear tem is obviously important in determining absolute rates of ET, in the following part the focus will be essentially placed on the electronic term where the bridge effects, the main subject of this review, are contained.

In a donor-bridge-acceptor (D-B-A) system, ET takes place as a single-step, coherent process from donor to acceptor. Nevertheless, the bridge plays an important kinetic role. In eq 2, H_{ET} is the electronic coupling between the reactant and product states of the ET process. According to the *superexchange* model[14] based on perturbation theory, bridge orbitals are involved in virtual states contributing to the electronic coupling between D and A subunits. Two main pathways can be effective in the superexchange mechanism for D-to-A ET (Figure 1): (i) an electron-transfer (ET) route, implying the intervening of lowest-lying virtual MOs centered on the bridge (the virtual state takes the form of D^{+}-B^{-}-A), and (ii) a hole-transfer (HT) pathway, which involves highest-lying occupied MOs centered on the bridge (with participation of a $D\text{-}B^{+}\text{-}A^{-}$ virtual state). If direct donor-acceptor coupling is negligible, the bridge-mediated superexchange coupling H_{ET} is given by eq 6.[8,14,15]

$$H_{ET} = H^e + H^h = \frac{H_{ie}H_{fe}}{\Delta E_{e(if)}} + \frac{H_{ih}H_{fh}}{\Delta E_{h(if)}} \quad (6)$$

In eq 6, H_{ih} and H_{fh} are the couplings between initial/final states and the $D\text{-}B^{+}\text{-}A^{-}$ HT virtual state, and H_{ie} and H_{fe} are the corresponding couplings with the D^{+}-B^{-}-A ET virtual state. The $\Delta E_{e(if)}$ and $\Delta E_{h(if)}$ terms in the denominator are the energy gaps between the ET or HT virtual states and the initial/final states of the process (such energy differences are univocally defined, as they refer to the transition state geometry, where the initial and final states are degenerate). According to eq 6, the relative weight of the ET and HT superexchange pathways depends inversely on the energy of the virtual states of the two types. In practice, the actual energy of the ET and HT virtual states will depend on the energy levels of the specific D-B-A system (e.g., with a MO energy level diagram as sketched in Figure 1, the two types of states would have similar energy). Thus, generally speaking, both ET and HT superexchange pathways should be considered for thermal ET processes.

3. Photoinduced electron transfer

The scheme in Figure 1, appropriate to describe the role of the bridge in thermal ET processes, cannot be simply applied when discussing *photoinduced* electron transfer (PET).

$$D\text{-}B\text{-}A + h\nu \rightarrow {}^*D\text{-}B\text{-}A \quad (7)$$
$${}^*D\text{-}B\text{-}A \rightarrow D^+\text{-}B\text{-}A^- \quad (8)$$
$$D\text{-}B\text{-}A + h\nu \rightarrow D\text{-}B\text{-}{}^*A \quad (9)$$
$$D\text{-}B\text{-}{}^*A \rightarrow D^+\text{-}B\text{-}A^- \quad (10)$$
$$D^+\text{-}B\text{-}A^- \rightarrow D\text{-}B\text{-}A \quad (11)$$

In this case, in fact, the relevant virtual states will depend not only on the specific energy levels of the system, but also on whether the PET is *oxidative* (eqs 7,8) or *reductive* (eqs 9,10) and on whether the forward charge separation (CS) step (eqs 8,10) or the backward charge recombination (CR) step (eq 11) are being considered. Since specific D-B-A systems may have substantially different energy level diagrams, generalizations should always be taken with caution. In the following discussion, however, we will refer to situations which are *usually* faced in D-B-A systems, and we will try to provide a series of simplified general arguments, hopefully of some practical value.

3.1 Oxidative PET

Let us first consider the case of *oxidative* PET (OPET, where excitation of the donor unit leads to transfer of an electron from the excited donor to the acceptor unit, i.e., to *oxidation* of the light-absorbing unit), as schematized in Figure 2, left half. For the CS reaction, virtual states potentially involved are only those connecting the initial *D-B-A photo-excited state (p) and the D^+-B-A^- CS state (s) through the bridge via two sequential one-electron transfer steps. The ET state D^+-B^--A (e) fulfills this requirement. A HT state of type D-B^+-A^- (h), on the contrary, would be related to the initial excited state by a two-electron movement, and thus cannot be considered as a superexchange mediator. A HT state containing an excited donor unit, *D-B^+-A^-, could in principle work, but its energy is expected to be so high that such a superexchange pathway can be safely neglected. In conclusion *oxidative photoinduced* CS is mediated via a *donor-to-bridge* ET pathway (Figure 2, left half). The superexchange electronic coupling matrix element for the oxidative CS process, H^{CS}_{OPET}, can be defined as in eq 12.

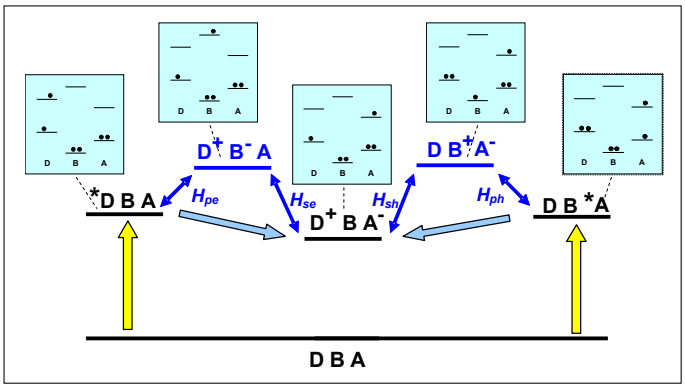

Fig. 2. Schematic representation of the superexchange interactions mediating PET in a D-B-A molecular dyad: *oxidative* ET following excitation of the donor (left); *reductive* ET following excitation of the acceptor (right). The yellow arrows represent light excitation and the light blue ones the CS processes. The various states (virtual states in blue) are sketched in terms of the associated electronic configurations (in the boxes). Couplings are represented by double arrows connecting the states. For further details, see text.

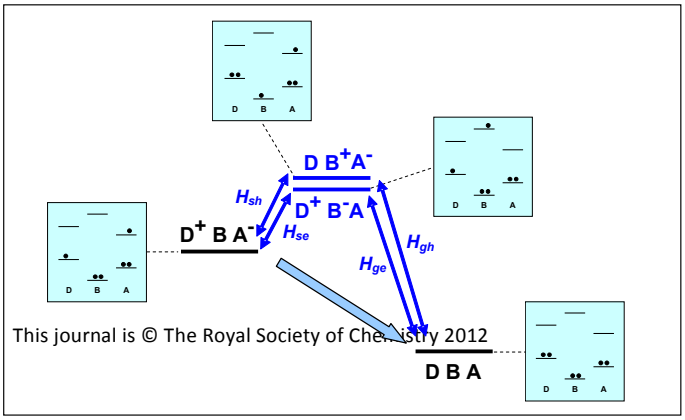

Fig. 3. Schematic representation of the superexchange interactions mediating CR in a D-B-A molecular dyad. The various states (virtual states in blue) are sketched in terms of associated electronic configurations in the boxes. Couplings are represented by double arrows connecting the states. For further details, see text.

$$H^{CS}_{OPET} = \frac{H_{pe}H_{se}}{\Delta E_{e(ps)}} \quad (12)$$

In eq 12, H_{pe}, H_{se} are the intermediate coupling matrix elements involving the ET virtual state as defined in Figure 2, left half and $\Delta E_{e(ps)}$ is the energy differences between the virtual states and the initial/final states of the process (degenerate at the transition-state nuclear geometry).

3.2 Reductive PET

Let us move to consider *reductive* PET (RPET, where excitation of the acceptor unit leads to transfer of an electron from the donor unit to the excited acceptor, i.e., to *reduction* of the light-absorbing unit). The situation is schematized in Figure 2, right half. Again, virtual states potentially involved are those connecting the initial D-B-*A photo-excited state (p) with the D^+-B-A^- CS state (s) through the bridge via one-electron transfer steps. In this case, the HT state D-B^+-A^- (h) fulfills the one-electron requirement, whereas an ET state of type D^+-B^--A (e) is ruled out by its two-electron character. Again, an ET state containing an excited acceptor unit, D^+-B^--*A, could in principle work, but its energy is expected to be so high that such a superexchange pathway can be safely neglected. In conclusion, reductive photoinduced CS is mediated via an *acceptor-to-bridge* HT (i.e., *bridge-to-acceptor* ET) pathway (Figure 2, right half). The superexchange electronic coupling matrix element for reductive CS, H^{CS}_{RPET}, can be defined as in eq 13, where H_{ph}, H_{sh}, are the intermediate coupling matrix elements and $\Delta E_{h(ps)}$ is the energy difference between the HT virtual state and the initial/final states of the process (degenerate at the transition-state nuclear geometry).

$$H_{RPET}^{CS} = \frac{H_{ph}H_{sh}}{\Delta E_{h(ps)}} \qquad (13)$$

3.3 Charge recombination (CR)

Regardless of whether the D^+-B-A^- CS state (s) is generated by oxidative or reductive PET, the CR (Figure 3) can be mediated by both ET, D^+-B^--A (e), and HT, D-B^+-A^- (h), virtual states involving the bridge. The appropriate superexchange electronic coupling matrix element for CR, H^{CR}, can be defined as in eq 14.

$$H^{CR} = \frac{H_{se}H_{ge}}{\Delta E_{e(gs)}} + \frac{H_{sh}H_{gh}}{\Delta E_{h(gs)}} \qquad (14)$$

where H_{ge}, H_{se}, H_{gh}, H_{sh} are the intermediate coupling matrix elements involving virtual states as defined in Figure 3, and $\Delta E_{e(gs)}$ and $\Delta E_{h(gs)}$ are the energy differences between the virtual states and the initial (s)/final (g) states of the process (degenerate at the transition-state nuclear geometry). The actual energies of the ET and HT virtual states, and thus the relative weights of the superexchange pathways, will depend on the energy levels of the specific D-B-A system (with a MO energy level diagram as sketched in Figure 3, the two types of states would have similar energy). Thus, generally speaking, both ET and HT superexchange pathways should be considered for CR processes.

4. Modular bridges

For bridges made of a given number of weakly interacting repeating units ("modular" bridges, often encountered in studies of distance dependence of ET), the above superexchange model must be slightly adapted. Considering, e.g., oxidative PET across a modular bridge of three repeating units the model becomes as depicted in Figure 4. The matrix element of the ET rate is given by eq 15.

$$H^e = \frac{H_{i1}H_{12}H_{23}H_{3f}}{\Delta E^3} \qquad (15)$$

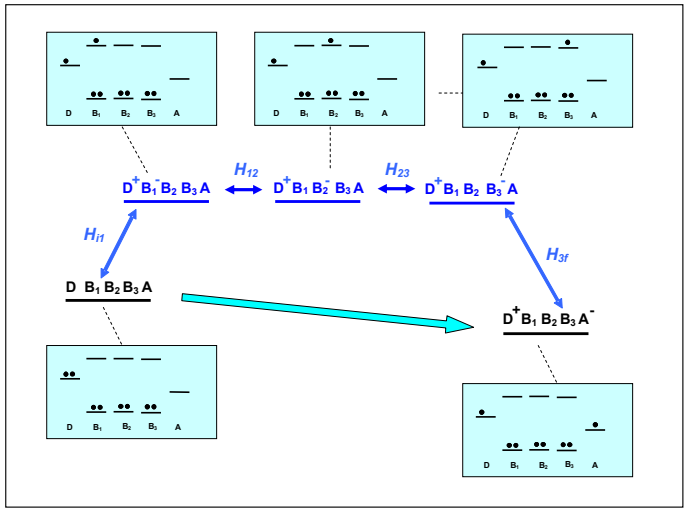

Fig. 4. Schematic representation of the superexchange interactions mediating oxidative PET in a dyad with donor and acceptor units connected by a three-module bridge. The various states (virtual states in blue) are sketched in terms of one-electron configurations in the associated boxes. Couplings are represented by double arrows connecting the states. For further details, see text.

In eq 15, H_{i1} and H_{3f} are the couplings between initial/final states and the bridge-localized states, $H_{12} = H_{23}$ are the inter-module couplings, and ΔE is the energy difference between the virtual states localized on the various units of the modular bridge and the initial (s) or final (g) states of the process (degenerate at the transition-state nuclear geometry). For the general case of n repeating units, with $H_{12} = H_{23} = \ldots = H_{mn}$

$$H^e = \frac{H_{i1}H_{nf}}{\Delta E}\left(\frac{H_{mn}}{\Delta E}\right)^{n-1} \qquad (16)$$

In eq 16, the first term of the product gives the coupling of the donor and acceptor units to the bridge and the second term yields the propagation of the interaction along the bridge. In the limit of weak interaction between the bridge subunits, ΔE is ideally considered to be constant, independent on bridge length.¶ This translates into an exponential fall-off of the electronic matrix element with the number of modules, n, in the bridge

$$H^e = H^e(0)\exp\left[-\frac{\beta_n}{2}(n-1)\right] \qquad (17)$$

where the pre-exponential factor $H^e(0)$ corresponds to the coupling for a single-module case

$$H^e(0) = \frac{H_{i1}H_{1f}}{\Delta E} \qquad (18)$$

and the decay coefficient β_n is given by

$$\beta_n = 2\ln\frac{\Delta E}{H_{mn}} \qquad (19)$$

The extension of the superexchange model from a single-unit bridge (eq 12, see Figure 2 left half) to modular bridges (eqs 15-19) is sketched in Figure 4 for an oxidative photoinduced electron transfer reaction (OPET). Appropriate schemes and expressions can be easily obtained, along the same lines, for the case of reductive photoinduced electron transfer (RPET) and CR.

Given eq 2, the superexchange model for ET through modular bridges predicts the frequently observed exponential fall off of ET rate constants with donor-acceptor distance r, shown in eq 20.

$$k^{ET} = k_0^{ET}\exp[-\beta(r - r_0)] \qquad (20)$$

$$\beta = \frac{2}{r_m}\ln\frac{\Delta E}{H_{mn}} \qquad (21)$$

In eq 20 β is expressed as in eq 21, where r_m is the length of the modular unit. Eq 21 points out that β depends, besides on the magnitude of the inter-module interaction, on the energy of the bridge-localized virtual states. Thus, bridges able to mediate

electron or hole transfer processes over large distances should generally have low-lying LUMOs or high-energy HOMOs. It has to be stressed, however, that ΔE in eq 21 is an energy difference between bridge-localized virtual states and initial/final states of the process, so that β may change, for a given modular bridge, by changing donor and acceptor units. Thus, although β is frequently used as a measure (in an inverse fashion) of the ability of the modular bridge as a mediator of donor-acceptor interactions, it is not, strictly speaking, an intrinsic property of the bridge.

5. Incoherent charge transport (hopping) through the bridge.

The superexchange model works under the assumption that the occupied and vacant energy levels of the bridge are far apart from those of the donor and acceptor units. In specific cases, this may not be true, leading to a substantial change in ET mechanism. If, for instance, the bridge LUMO happens to be at an energy similar or lower than that of the donor (Figure 5a), the bridge-localized ET state is not anymore a virtual state, but rather a real, thermodynamically accessible state. In this case,

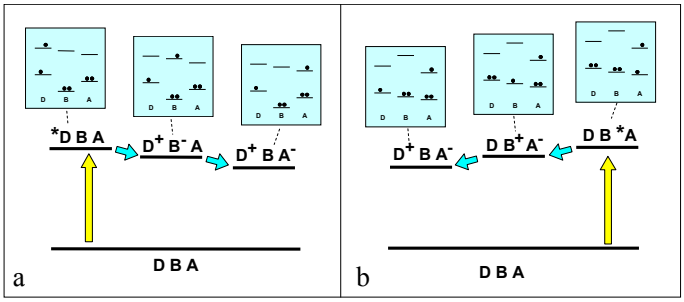

Fig. 5. Schematic representation of D-B-A systems characterized by low-lying bridge-localized states, where *oxidative* (a) or *reductive* ET (b) take place by an incoherent hopping mechanism. The various states (virtual states in blue) are sketched in terms of one-electron configurations in the associated boxes. Couplings are represented by double arrows connecting the states. For further details, see text.

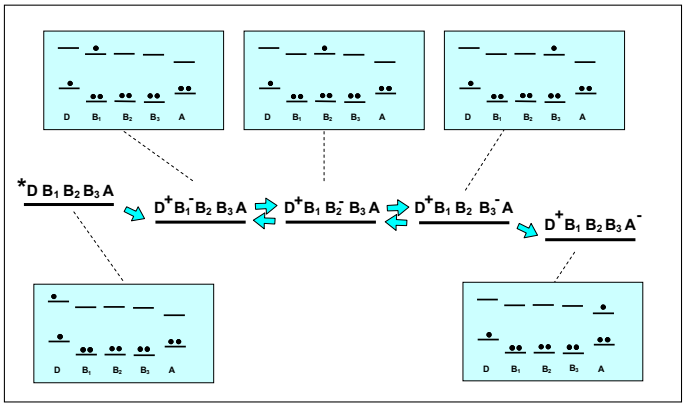

Fig. 6. Schematic representation of an injection-hopping-trapping mechanism for *oxidative* PET from donor to acceptor through a three-unit modular bridge. The initial, final, and intermediate states are sketched in terms of one-electron configurations in the associated boxes. For further details, see text.

oxidative PET proceeds as an incoherent two-step charge transport process (electron hopping) through the bridge. If, on the other hand, the bridge HOMO happens to be at an energy similar or higher than that of the donor (Figure 5b), the bridge-localized HT becomes a real, thermodynamically accessible state and reductive PET proceeds as an incoherent two-step charge transport process (hole hopping) through the bridge. In terms of rates, hopping mechanisms are obviously expected to drive much faster ET processes than superexchange.

Such a change in mechanism has interesting consequences, in the case of a modular bridge, on the expected distance dependence of ET rates. When the ET or HT states of the modular bridge are thermodynamically accessible from the photoexcited donor or acceptor, the process occurs by (i) electron or hole injection into the bridge, (ii) random, reversible hopping between degenerate modular units, and (iii) irreversible trapping by the acceptor.[15a] This is illustrated in Figure 6, for the case of oxidative PET (appropriate schemes can be easily obtained, along the same lines, for the case of reductive photoinduced CS and CR). In such injection-hopping-trapping mechanisms, a weak distance dependence of rates is expected, of the type

$$k^{ET} \propto n^{-\eta} \qquad \eta \approx 1-2 \qquad (22)$$

where n is the number of modules in the bridge.[16] Clearly, modular bridges able to undergo electron/hole injection from excited donor/acceptor are particularly well-suited for long-range charge transport. In such a situation, the bridges can be considered to behave as true "molecular wires" connecting donor and acceptor.

6. Discussion

The above general introduction summarizes the essential conceptual framework to describe the role of the bridge in PET in donor-bridge-acceptor systems. The emerging picture is a rather complex one, where a variety of structural and energetic factors of the whole D-B-A system play relevant roles in determining rates and efficiencies. In this discussion, selected examples from the extensive literature on PET in D-B-A systems are chosen to illustrate specific mechanistic aspects of the problem. The choice of the examples and the level of discussion is mainly determined by tutorial aims. Thus, for each system, the description will be limited to essential results relevant to exemplify the specific mechanistic point. For more detailed accounts and discussions, the reader is referred to the original references.

6.1 Manipulation of superexchange couplings by bridge substitution.

The first demonstration of how ET rates can be controlled by manipulation of superexchange couplings via the energy of bridge-localized virtual states was provided in 1989 by Wasielewski *et al.*, by comparing the behavior of dyads **1** and **2**.[17] Among more recent cases, dyads **3** and **4**,[18] and **5** and **6**[19] can be also taken as useful examples. In **1**, **2**, **3**, and **4**, oxidative ET is induced by excitation of the zinc porphyrin donor. In **5** and **6**, thermal ET from the phenothiazine donor to the Ru(III) acceptor is triggered by bimolecular photochemical oxidation of the original Ru(II) unit with an external acceptor. In going from **1** to **2**, the application of methoxy substituents on the central benzene ring of the spacer makes the bridge easier to oxidize, and thus lowers the D-B$^+$-A$^-$ HT virtual state. The consequence is an acceleration of the CR process (from 1.4×10^{10} s^{-1} to 5.0×10^{10} s^{-1}) while CS, that cannot be mediated by this type of virtual state, remains appreciably constant (from 8.2×10^{9} s^{-1} to 8.5×10^{9} s^{-1}).[17] A similar, and more pronounced effect is observed upon extensive substitution of methyl groups with methoxy groups along the modular bridge of dyads **5** and **6**.[19] Again, the lowering of the D-B$^+$-A$^-$ HT states, which for oligophenylene bridges constitutes the dominant superexchange pathway, brings about a large increase in ET rate (from 5.0×10^{4} s^{-1} to 5.9×10^{7} s^{-1}).

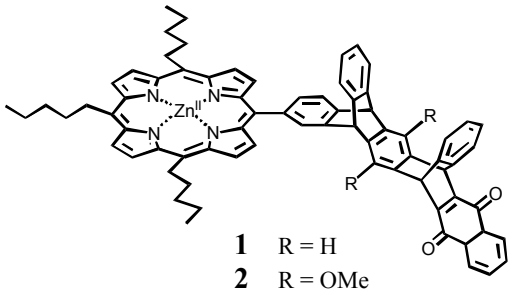

1 R = H
2 R = OMe

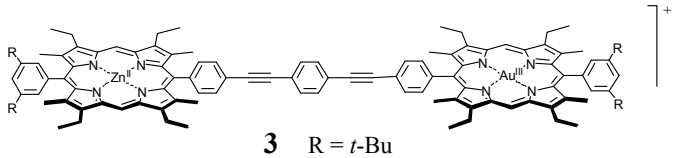

3 R = *t*-Bu

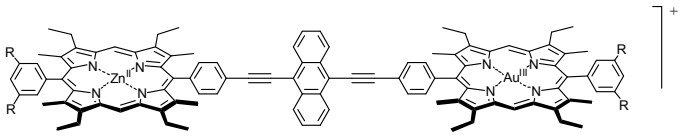

4 R = *t*-Bu

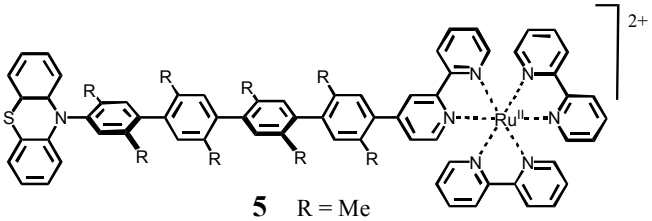

5 R = Me
6 R = OMe

The case of dyads **3** and **4** is a somewhat different one, in that the manipulation of superexchange couplings is obtained by inserting different aromatic hydrocarbon units in the central position of the bridge.[18] Here, the effect of changing the central group from benzene to the more delocalized anthracene is to lower the LUMO and to lift the HOMO level of the bridge, thus affecting both CS (that goes from 2.5×10^{9} s^{-1} to 3.0×10^{10} s^{-1}) and CR (that goes from 1.7×10^{8} s^{-1} to 2.7×10^{8} s^{-1}). A particularly useful feature of these systems is that CS and CR have very similar driving forces, both closely matching the reorganization energy. Therefore nuclear factors are the same for the two processes, and the reasons for CS being always much faster than CR must be sought exclusively in differences in electronic factors. The relevant expressions are eq 12 for CS and eq 14 (mainly HT term) for CR. Interestingly, quantitative evaluation[18] shows that, aside from differences in the ΔE values of the relevant virtual states, the differences in rates of CS and CR are largely determined by differences in donor-bridge-acceptor couplings ($H_{pe}H_{se}$ in eq 12 for CS *vs.* $H_{sh}H_{gh}$ in eq 14 for CR). The reasons for such a difference can be qualitatively understood considering that (i) in CS, the interaction between the bridge and the zinc porphyrin takes place at the LUMO level (H_{pe}, Figure 2) whereas in CR occurs at the HOMO level (H_{sh}, Figure 3), and (ii) at the *meso* positions where the bridge is connected, the zinc porphyrin LUMO has substantial amplitude whereas the HOMO has nodes.[18]

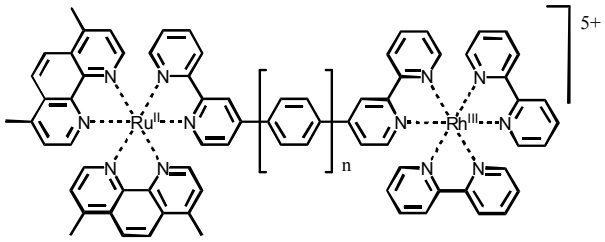

7(1) n = 1
7(2) n = 2
7(3) n = 3

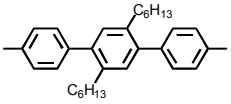

7(3')

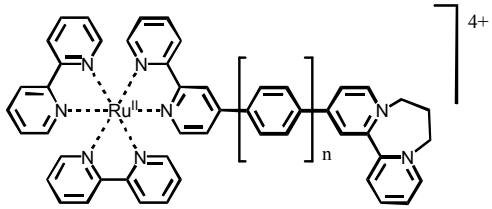

8(1) n = 1
8(2) n = 2
8(3) n = 3
8(4) n = 4
8(5) n = 5

6.2 Relative rates of charge separation and recombination.

A series of studies of oxidative PET in dyads involving a Ru(II) polypyridine unit as photoexcitable donor, a Rh(III) polypyridine unit[20] or a quaternarized bipyridine (DQ^{2+})[21] as acceptor, and bridges of the oligo *p*-phenylene type, can be used to exemplify some specific points mentioned in the general introduction. For all **7(n)** dyads, excitation of the Ru(II) polypyridine unit is followed by ET to the Rh(III) unit, i.e, by oxidative quenching. The rate constants, obtained from emission lifetimes, are: **7(1)**, 3.0×10^{9} s^{-1}; **7(2)**, 4.3×10^{8} s^{-1}; 7**(3)**, 1.0×10^{7} s^{-1}; **7(3')**, 1.1×10^{6} s^{-1}. They are relatively slow, consistent with the weak exergonicity of the process (ΔG = −0.05 eV), and undergo a general decrease with increasing distance (i.e., number of *p*-phenylene spacers), as expected on the basis of Figure 4 and eqs 17,20. The decay in rate constants with distance for **7(1)**, **7(2)**, **7(3)** is appreciably exponential (Figure 7), with a β value of ca. 0.65 $Å^{-1}$.

Interestingly, the rate constant for **7(3')**, which only differs from **7(3)** for the presence of two hexyl substituents on the central phenylene ring, is lower by one order of magnitude than that of the unsubstituted analogue.

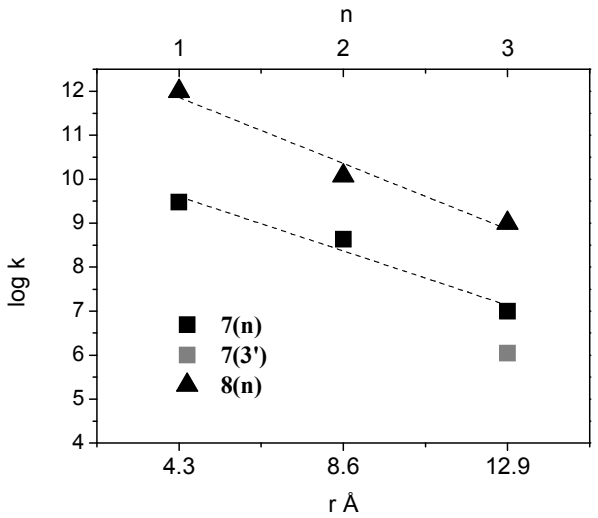

Fig. 7. Distance dependence of the rate constants for oxidative PET in dyads **7(n)** (squares) and **8(n)** (triangles).

The reason of this behavior is easily understandable from eq 15, where the donor-acceptor coupling H^e depends on the electronic couplings between adjacent modules in the bridge, H_{mn}. With oligophenylene bridges this is a sensitive function of the twist angle between adjacent modules.[22,23] Alkyl substitution at the central ring causes increased steric hindrance, increased twist angle and decreased electronic coupling between adjacent units of the bridge. This translates into a decrease in the overall superexchange coupling and into a drastic slowing down of the ET process (with a simple cos^2 dependence on twist angle, an increase upon alkyl substitution from ca. 20° to ca. 60° could easily account for the observed difference). In the series of dyads **8(n)**, involving the better bipyridinium acceptor, oxidative quenching (ΔG = −0.33 eV) is generally much faster: **8(1)**, 1.0×10^{12} s^{-1}; **8(2)**, 1.2×10^{10} s^{-1}; **8(3)**, 1.0×10^{9} s^{-1}; **8(4)**, 8.1×10^{8} s^{-1}; **8(5)**, 3.7×10^{8} s^{-1}. Considering the data for n = 1-3 (for n = 4-5 a different, reductive quenching mechanism[21] operates), the distance dependence is again exponential, with a similar[§] β value (0.78 $Å^{-1}$). As pointed out above, the prediction of exponential decay in rates with bridge length relies on the assumption that the energy of the ET virtual states (ΔE, in eq 21) remains constant along a given series of dyads. Strictly speaking, this is not true for the oligo *p*-phenylene bridges, where increasing conjugation leads to decreasing LUMO and increasing HOMO energies.[‡] The experimental observation of an appreciably exponential decay simply means that the changes in the energy of the ET virtual states with bridge length are not large enough to have a major effect on β.[†,#]

The relationship between CS and CR in the **7(n)** and **8(n)** series of dyads is worth of comment. In all **7(n)** dyads, oxidative quenching is followed by faster CR, with no accumulation of observable ET products in time-resolved experiments. Relative rates of CS and CR can, in principle, be determined by both nuclear and electronic factors (*FCWD* and H_{ET}, respectively, in eq 2). For the **7(n)** series, the nuclear factors could account, at least partially, for the observation of CR faster than CS: in fact, the high reorganization energy of the Rh(III)/Rh(II) couple[24] should favor the highly exergonic CR (ΔG = −2.00 eV) over the slightly exergonic CS (ΔG = −0.05 eV). In the **8(n)** series, the behavior is more complex. In fact, with **8(1)** very fast oxidative quenching (k = 1.0×10^{12} s^{-1}) is followed by a detectable, slower CR (k = 2.7×10^{11} s^{-1}). The relative rates of CS and CR can be explained here, at least partially, by nuclear factors, as the reorganization energy of the DQ^{2+}/DQ^{+} couple is small, CS is now substantially exergonic (ΔG = −0.33 ± 0.02 eV) and CR (ΔG = −1.72 ± 0.02 eV) is likely to lie deep into the Marcus inverted region. On passing to dyads **8(2)** and **8(3)**, the energetics (reorganization energy, driving forces) remain practically the same. This not withstanding, no appreciable accumulation of transient ET products takes place after oxidative quenching, implying that CR has become faster than CS. Clearly, electronic factors play here a crucial role. As discussed above (Figures 2 and 3) CS and CR processes follow superexchange pathways involving different types of virtual states: for oxidative CS, ET D^{+}-B^{-}-A states; for CR, in principle, both ET and HT states. In practice, with oligo *p*-phenylene bridges, where HT states are much lower in energy than ET ones,[‖] CR takes place by a D-B^{+}-A^{-} HT superexchange pathway. Upon bridge elongation, both types of virtual states undergo a decrease in energy, but the decrease of the HT states is relatively much larger than that of the ET ones.[‖,**] Thus, while the assumption of constant ΔE in eq 15,16 may approximately hold for CS,[†] it is far from being obeyed for CR. The decrease in energy of the HT virtual states, and the consequent increase in superexchange coupling (eq 16), is likely to partially compensate for the distance effect, yielding a distance dependence for CR smoother than that observed for CS. In summary, the different superexchange mechanisms involved in CS and CR, and their different distance

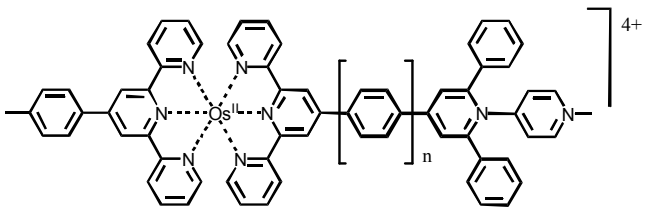

9(1) n = 1
9(2) n = 2

dependence, determine the inversion in relative rates of the two processes observed between **8(1)** and **8(2)**.

A related case is that of dyads **9(1)** and **9(2)**. Upon excitation of the Os(II) polypyridine chromophore, dyad **9(1)** exhibits a rate constant for PET to the bipyridinium acceptor of 1.4×10^{11} s^{-1}, and a rate constant for CR of 2.2×10^{10} s^{-1}.[25,26] Since the driving force ΔG^0 for ET from the triplet metal-to-ligand charge-transfer (MLCT) excited state of the Os(II) polypyridine chromophore (that is the lowest-energy excited state of the Os-based subunit) to the bipyridinium acceptor subunit is −0.25 eV and that for CR leading to the ground state is −1.47 eV, the first process is likely to lie in the "normal" region and the latter in the "inverted" region of Marcus theory. This can justify the slower rate of CR relative to photoinduced CS in **9(1)**. The comparison with the related species **9(2)**,[25] is interesting. In dyad **9(2)** the forward ET process ($k = 1.5\times10^{10}$ s^{-1}) is slower than in **9(1)**, as expected as a consequence of the increased donor-acceptor distance. But again, in **9(2)** the CR reaction is faster than CS, with no appreciable transient accumulation of ET products. This means that, in going from **9(1)** to **9(2)**, CR is not slowed down to the same extent as CS. Again, the reason for this behavior lies in the fact that a biphenylene bridge is much easier to oxidize than a phenylene one.[‡] The energy of the D-B^+-A^- state decreases significantly upon bridge extension, leading, in a HT superexchange mechanism, to an acceleration of CR that largely compensates for the increased distance effect.

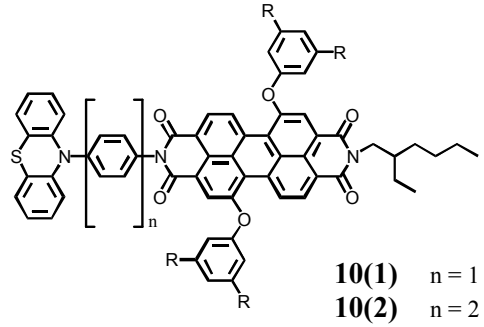

10(1) n = 1
10(2) n = 2
10(3) n = 3
10(4) n = 4
10(5) n = 5

R = *t*-Bu

The discussion of systems such as **7(n)**, **8(n)** and **9(n)** shows that oligo *p*-phenylene bridges have a substantial drawback from the viewpoint of achieving efficient, long-lived CS *upon donor excitation* in D-B-A dyads. These bridges are characterized by relatively high-energy filled orbitals and, in terms of electronic couplings, this will generally favor CR (mediated by D-B^+-A HT virtual states) relative to CS (mediated by D^+-B^--A ET virtual states). It is important to realize, however, that this conclusion only holds for CS and CR following *oxidative* electron transfer quenching (OPET). In fact, when the same type of bridges are involved in *reductive* photoinduced electron transfer (RPET), the behavior is quite different. For example, in dyads **10(n)** (n = 1-3),[27] excitation of the perylenebisiimide chromophore is followed by a very fast ET from the phenothiazine donor unit and a much slower CR of the transient CS products. In particular, photoinduced CS occurs with rate constants of 5.2×10^{10} s^{-1}, 4.2×10^{9} s^{-1}, and 6.2×10^{8} s^{-1} for **10(1)**, **10(2)** and **10(3)**, respectively, whereas rate constants for CR are 8.6×10^{8} s^{-1} for **10(1)**, 4.8×10^{7} s^{-1} for **10(2)**, and 3.0×10^{6} s^{-1} for **10(3)**. On increasing the number of bridge phenylene rings, the usual exponential dependence of ET rate on distance is qualitatively followed by both forward (β = 0.46 $Å^{-1}$) and backward processes (β = 0.67 $Å^{-1}$), with CS remaining faster than CR by ca. two orders of magnitude along the whole n = 1-3 series.[27] Therefore, formation of ET products is always efficient upon reductive photoinduced electron transfer (RPET) in the **10(n)** dyads. Unlike the oxidative quenching case, here both reductive CS (Figure 2) and CR (Figure 3) are mediated by the same type of D-B^+-A^- HT virtual states, implying relatively similar superexchange electronic couplings for the two processes. Thus, the large differences in rates of CS and CR are mainly given by differences in nuclear factors (ΔG, normal *vs.* inverted Marcus region) of the two processes. In conclusion, the easily oxidizable nature of the oligo *p*-phenylene bridges, which was detrimental to long-lived CS upon oxidative quenching of the donor unit, turns out to be advantageous when CS is obtained by reductive quenching of the acceptor unit. Interestingly, for more extended dyads of the **10(n)** series (n = 4,5), the D-B^+-A^- HT states become so low in energy as to induce a change in mechanism, for both CS and CR, from coherent ET to incoherent injection/hopping.[27]

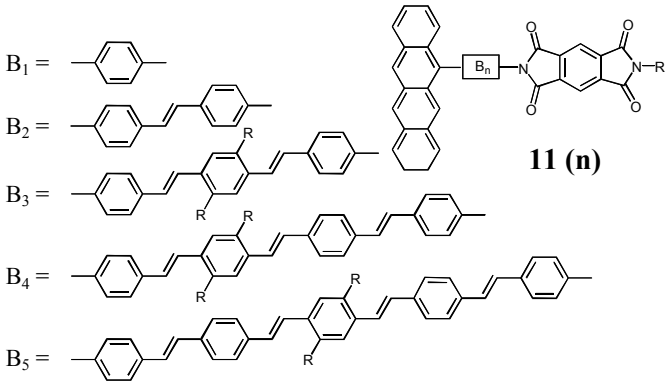

11 (n)

6.3. Switching mechanism from superexchange to injection.

A very clear case of switch in mechanism from superexchange to charge injection is that reported by Wasielewsky *et al.*[28] with the series of dyads **11(n)**. These dyads consist of a tetracene donor and a pyromellitimide acceptor linked by oligo *p*-phenylenevinylene bridges of various length.

In all the dyads, efficient oxidative PET is observed following excitation of the tetracene unit. The distance-dependence of the rates is, however, very peculiar (Figure 8): from **11(1)** to **11(2)** the rate decreases as expected (with an apparent β of ca. 0.27 Å^{-1}) but then in going to **11(3)** an abrupt *increase* in rate occurs, followed by a much shallower decay for **11(4)** and **11(5)** (apparent β of only 0.04 Å^{-1}). The rationale for this sharp change in behavior lies in the strong decrease in energy experienced, as the bridge is extended, by the LUMO of the oligo *p*-phenylenevinylene bridges. For **11(1)** and **11(2)** D^+-B^--A ET states involving the bridge are high in energy and play

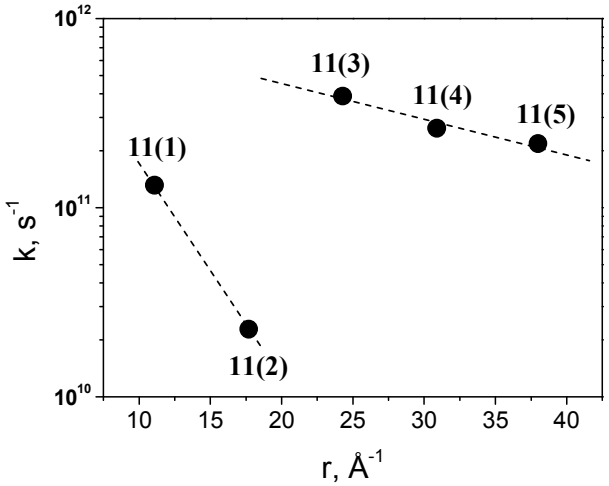

the usual role of virtual states mediating a superexchange mechanism (cfr. Figure 4 and eqs 15-21). But for **11(3)**, and even more so for **11(4)** and **11(5)**, the D^+-B^--A states become sufficiently low in energy so as to allow electron injection into the bridge from the *D-B-A excited state (cfr. Figure 6 and eq 22). Thus, the sharp change in kinetics observed in Figure 8 reflects the switch in behavior of the oligo *p*-phenylenevinylene bridge with length from a superexchange mediator to a molecular wire behavior.[28]

Fig. 8. Distance dependence of OPET in dyads **11(n)**. Adapted from ref. 28.

6.4 Distance dependence: how bridge-specific is the parameter β.

It was pointed out above in several instances that the β parameter (eqs 20,21), describing the exponential decay of ET rates with bridge elongation, is not strictly speaking a bridge-specific parameter. A very clear demonstration is provided by the behavior of dyads **12(n)** (with n = 1-5) and **13(n)** (with n = 1-4). In dyads of type **12(n)**, photoexcitation of the Re(I) acceptor complex is followed by reductive ET from the phenothiazine donor.[29] In dyads of type **13(n)**, on the other hand, bimolecular photochemical oxidation of the Ru(II) metal complex unit by an external acceptor is used to trigger thermal ET from the phenothiazine donor to photogenerated Ru(III) acceptor.[30] In both cases, the ET process is mediated by HT states (obviously for reductive quenching of **12(n)**, for energy

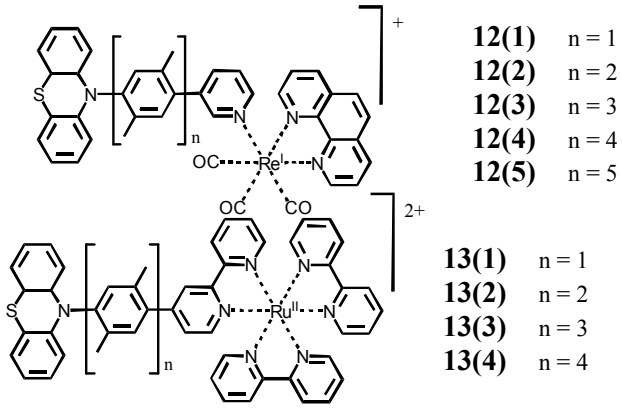

reasons with this type of bridges for the thermal process in **13(n)**). When the distance dependence of the two ET processes is compared (Figure 9), the evident result is that the slope of the exponential plots is definitely steeper for dyads **13(n)** (β = 0.77 Å^{-1}) than for dyads **12(n)** (β = 0.52 Å^{-1}). This difference can be easily understood in terms of eq 6 (dominated by the HT term, for superexchange coupling with this type of bridges), considering the energetics of ET within the two series. Actually, the members of the two sets of dyads are identical in donor and bridge units but differ in the acceptor, which is an excited Re(I) complex in **12(n)** and an oxidized Ru(III) species in **13(n)**. Since the excited Re(I) complex is a better electron acceptor (by ca. 200 mV) than the Ru(III) complex, the energy of the D-B^+-A^- virtual states is higher in the latter case than in the former one. Therefore, with a larger ΔE term in eq 21, a larger β value is expected for dyads **13(n)** relative to dyads **12(n)**. The different distance dependence obtained with these two classes of dyads shows very clearly that β is not a bridge-specific, but rather a system-dependent parameter. A common

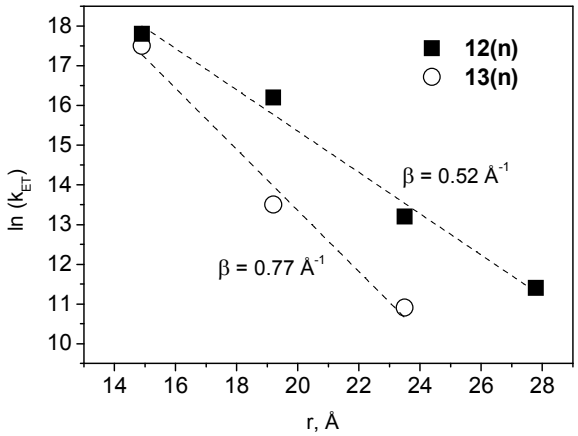

Fig. 9. Exponential decay of ET rate constants with donor-acceptor distance in dyads **12** and **13**. Adapted from ref. 30.

conception is that the ability of a bridge to mediate ET over large distance depends on the degree of conjugation within the

bridge. This conception, that implicitly emphasizes the effect of inter-module couplings (H_{mn} in eq 21) on the overall superexchange interaction, remains a useful generalization when comparing different types of bridge. It neglects, however, the effect of the energy difference between bridge-localized virtual states and the initial/final states (ΔE in eq 21). The above discussed experiments demonstrate that, in fact, with a given type of bridge significant changes in β values can be obtained depending on the actual donor and/or acceptor units.

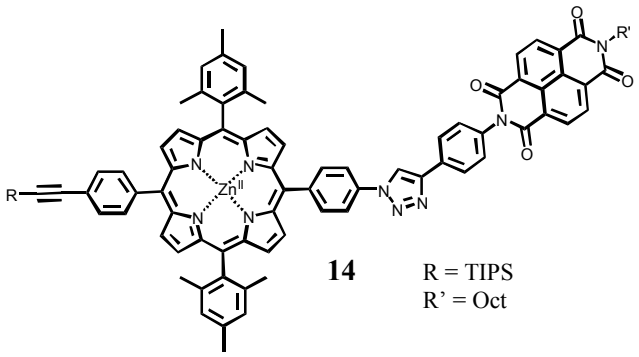

14 R = TIPS
R' = Oct

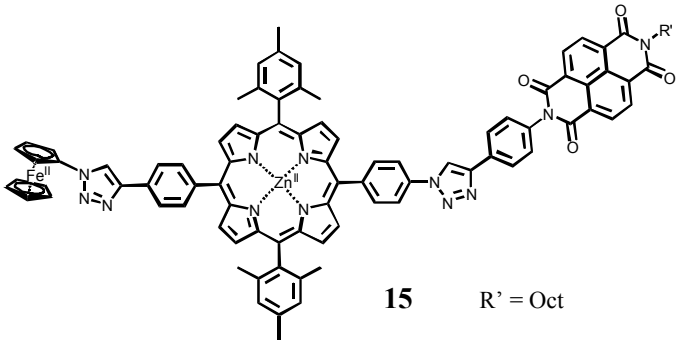

15 R' = Oct

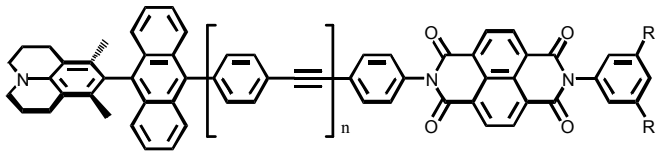

16(1) n = 1
16(2) n = 2
16(3) n = 3

R = *t*-Bu

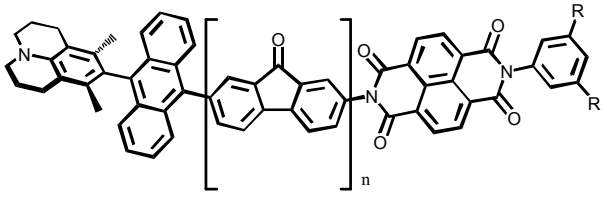

17(1) n = 1
17(2) n = 2
17(3) n = 3

R = *t*-Bu

6.5 Oxidative and reductive PET: electron and hole transfer pathways.

Cases in which, in a single D-B-A system, CS is obtained by excitation of both donor and acceptor units are rare. One of such cases is represented by dyad **14**, where the donor unit is a zinc porphyrin (ZnP) and the acceptor unit is a naphthalene bisimide (NDI), and by the related triad system **15** including ferrocene as a secondary electron donor.[31] The dyad system **14** exhibits relatively inefficient quenching of the ZnP singlet excited state, slow CS (1.1×10^8 s^{-1}) to yield ZnP^+-NDI^- and fast CR (> 10^9 s^{-1}) processes. Excitation of dyad **14** in the NDI chromophore, on the other hand, leads to very fast (> 7×10^{10} s^{-1}) and efficient CS. This strong difference in behavior is reflected in the performance of the triad **15**, where the long-range, μs-lived CS state Fc^+-ZnP-NDI^- is formed much more efficiently upon NDI than ZnP excitation. Although this difference in rates and efficiencies can be partially justified by the different driving force of the oxidative and reductive CS processes, electronic factors are likely to play a substantial role as well. In particular, as predicted by Figures 2, following donor excitation CS takes place at the LUMO level, with superexchange mixing involving ET virtual states of the bridge, whereas upon excitation of the acceptor CS takes place at the HOMO level, with superexchange mixing involving HT virtual states of the bridge. In this specific case, as shown by DFT calculations, the HOMO of the phenyltriazole bridging unit actually lies *higher* in energy than that of the NDI acceptor.[31] In other words, the HT state, rather than a virtual state for superexchange, becomes a real intermediate in a D→B→A electron cascade at the HOMO level (cfr. Figure 5b).

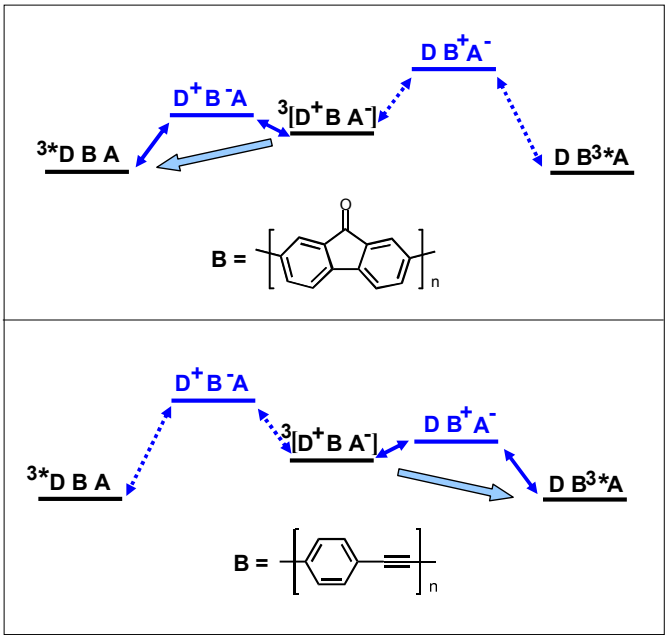

Fig. 10. Schematic representation of the pathways available to dyads of type **16** (lower panel) and **17** (upper panel) for CR of the triplet CS state to local triplet

excited states. Qualitative energy level diagram, emphasizing the relationship between the relative energies of ET and HT virtual states ad the preferred CR to donor or acceptor local triplets. For detailed energetics and further information, see original reference.[32]

A particularly clear demonstration of the relevance of bridge energetics for superexchange mediation of oxidative and reductive excited-state ET processes has been provided by Wasielewski *et al.*[32] in recent studies of CR in dyads **16(n)** and **17(n)**. In these dyads the donor is 3,5-dimethyl-4-(9-anthracenyl)-julolidine, the acceptor is naphthalene-1,8:4,5-bis(dicarboximide), while the bridges are either oligo(*p*-phenyleneethynylene) (**16(n)**) or oligo(2,7-fluorenone) (**17(n)**). In both types of dyads, excitation of the donor is followed by fast and efficient oxidative ET. The CS state, initially produced with singlet spin multiplicity, undergoes rapid radical pair intersystem crossing to yield a triplet CS state, $^3[D^+\text{-B-}A^-]$. Subsequent CR is spin selective, i.e., the triplet CS state recombines to yield, rather than the ground state, a locally excited triplet state. This can take place in two ways, leading alternatively to the triplet state of the donor, ^{3}*D-B-A, or to that of the acceptor, D-B-^{3}*A. The situation, as depicted schematically in Figure 10, aside from the reversal in energy ordering of CS and local excited states, and thus in the direction of the processes, is conceptually similar to the standard picture for *oxidative* and *reductive* PET (Figure 2). In particular, CR leading to the triplet of the donor must be mediated by ET virtual states, whereas that leading to the triplet state of the acceptor should follow a HT superexchange pathway. As a matter of fact, a detailed study of these systems carried out by means of time-resolved electron paramagnetic resonance (TREPR) spectroscopy has shown that CR takes place preferentially to the acceptor triplet when the bridge is an oligo(*p*-phenyleneethynylene) (**16(n)**), while it occurs preferentially to the donor triplet when the bridge is an oligo(2,7-fluorenone) (**17(n)**).[32]

The selectivity of the two bridges in directing CR can be easily understood on the basis of a superexchange mechanism (eq 6) by considering the relative energies of the HT and ET virtual states. With the oligo(*p*-phenyleneethynylene) bridges (**16(n)**), the HT virtual states are lower in energy than the ET ones by ca. 0.5 eV, and thus the HT superexchange pathway leading to acceptor triplet is favored. In the case of the oligo(2,7-fluorenone) bridges (**17(n)**), the energy situation is essentially reversed, and the donor triplet is formed by an ET superexchange pathway.[32]

6.6. Mixed-valence systems

Finally, it should be pointed out that some of the arguments used here to discuss superexchange-assisted ET in D-B-A systems can also be applied to discuss the role played by the bridge in mixed-valence systems. This subject, which constitutes itself a wide and interesting research field,[33-35] is just mentioned here to the purpose of stressing some analogies. In mixed-valence systems, schematically indicated as M-B-M'$^+$, two redox centers in different oxidation states (often but not necessarily transition metals, often but not necessarily identical) are connected by a bridge. Such systems are characterized by the appearance of optical intervalence transfer (IT) transitions (eq 23), and the analysis of such transitions

$$\text{M-B-M'}^+ + h\nu \rightarrow \text{M}^+\text{-B-M'} \qquad (23)$$

according to the Hush theory[36] affords a straightforward way to measure the electronic coupling between the redox centers. The relationship between the metal-metal coupling and the experimental parameters of the IT band is given by eq 24

$$H_{MM'} = \frac{2.05\times10^{-2}\sqrt{\bar{\nu}\,\Delta\bar{\nu}_{1/2}\,\varepsilon_{max}}}{r_{MM'}} \qquad (24)$$

where H_{MM} is the metal-metal coupling (in cm^{-1}), ε_{max} is the maximum extinction coefficient for the IT transition, ν is its energy and $\Delta\nu_{½}$ is its full-width at half-maximum (FWHM, in cm^{-1}), and $r_{MM'}$ is the metal-metal distance. Thus, many of the bridge effects discussed in the previous sections for ET rates can be verified, with appropriate mixed-valence systems, in terms of spectroscopically determined electronic couplings.

For instance, the exponential decay of donor-acceptor coupling with distance (eq 17) can be checked by looking at the IT band intensity of mixed-valence systems involving modular bridges of variable length.[33] Of particular interest in this respect is the possibility to examine highly delocalized bridges, which would hardly lie in the superexchange regime if studied by conventional photoinduced ET processes. As an example, with the series of mixed-valence complexes **18(n)** studied by Launay *et al.*,[37] the analysis of the IT bands using eq 24 yielded a very low experimental β value of 0.07 Å^{-1}. It should be mentioned that such studies are complicated by the fact that IT bands may become very weak at long distances and often have to be deconvoluted from other more intense (e. g., metal-to-ligand charge transfer) transitions. Systems with organic

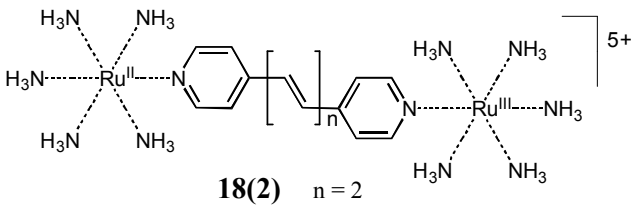

18(2) n = 2
18(3) n = 3
18(4) n = 4

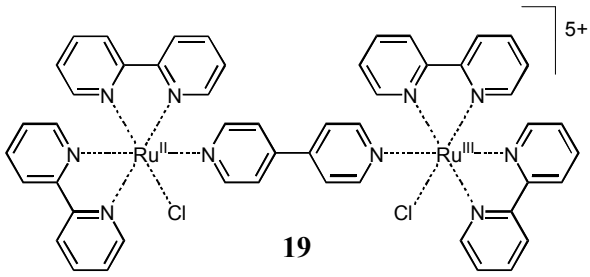

19

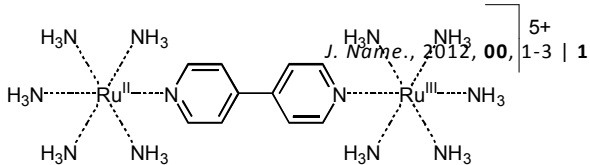

molecules replacing metal complexes as terminal units, such as, e.g., the triarylamine-based mixed-valence systems studied by Lambert and Nöll,[38] are relatively free from these drawbacks and permit a better definition of the distance-dependence of electronic couplings.

An interesting comparison is that between mixed-valence systems **19**[39] and **20**.[40] While in both cases the IT transition involves Ru(II) and Ru(III) centers bridged by a 4,4'-bipyridine ligand, the band intensities of the two systems are widely different, indicating a much weaker metal-metal coupling for **19** than for **20**. In an ET superexchange mechanism, this can be attributed to the effect of π-acceptor ancillary ligands in **19** that (i) make the Ru(II) more difficult to oxidize and thus lift the energy of the ET to the bridge virtual state (ΔE in eq 16) and (ii) decrease, by competitive π back-bonding, the metal-bridge interaction (H_{i1} and H_{nf} in eq 16). This points out again the dependence of superexchange coupling not only on the bridge but also on the donor and acceptor units.

A nice experimental example of the effect of couplings between adjacent units in modular bridges is provided by the series of mixed-valence dyads **21(n)**, studied by Harriman *et al*.[41] In these dyads, the torsion angle of the central biphenylene unit of the bridge is modulated by the length of the oligo-methylene strap, spanning the range 37-94° with n = 1-4. This is reflected in the intensity of the IT band that, when analyzed in terms of Hush theory (eq 24), yields $H_{MM'}$ values ranging from 86 to 57 cm^{-1}. Again, this is a clear, direct demonstration of how the donor-acceptor couplings are affected by inter-module couplings (H_{mn} in eq 16).

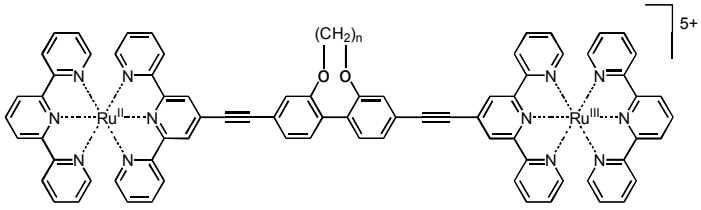

21(1) n = 1
21(2) n = 2
21(3) n = 3
21(4) n = 4

Finally, it is interesting to point out that in mixed-valence systems ET and HT states involving the bridging ligand (i.e., the same states considered as virtual states in superexchange coupling) are often *spectroscopically* accessible, in the form of metal-to-ligand (MLCT) or ligand-to-metal (LMCT) absorption bands. As pointed out by Creutz, Newton, and Sutin,[42a] a Hush-type analysis of such spectral transitions affords a direct measurement of the metal-bridge electronic couplings, and such couplings can be used to calculate the metal-metal interaction, in a superexchange formalism similar to that of eq 6 (eq 25)[33,42]

$$H_{MM'} = \frac{H_{ML}H_{M'L}}{\Delta E_{ML}} + \frac{H_{LM}H_{LM'}}{\Delta E_{LM}} \qquad (25)$$

where the effective energy gaps can be obtained from spectroscopic measurements (eqs 26,27).

$$\Delta E_{ML} = \left[\frac{1}{2}\left(\frac{1}{\Delta E_{MLCT}} - \frac{1}{\Delta E_{MLCT} - \Delta E_{IT}}\right)\right]^{-1} \qquad (26)$$

$$\Delta E_{LM} = \left[\frac{1}{2}\left(\frac{1}{\Delta E_{LMCT}} - \frac{1}{\Delta E_{LMCT} - \Delta E_{IT}}\right)\right]^{-1} \qquad (27)$$

For instance in compound **20**, besides an IT band (1030 nm, ε_{max} = 920 $M^{-1}cm^{-1}$) also a Ru(II) → 4,4'-bpy metal-to-ligand charge transfer (MLCT) band is observed (526 nm, ε_{max} = 12600 $M^{-1}cm^{-1}$). In this case, analysis of the MLCT band yields $H_{ML} = H_{M'L} = 4.4\times10^3$ cm^{-1} and $\Delta E_{MLCT} = 12.7\times10^3$ cm^{-1}. The value of metal-metal coupling calculated with these parameters from eq 25, assuming a prevailing ET superexchange pathway, is $H_{MM'} = 0.8\times10^3$ cm^{-1}, in satisfactory agreement with the experimental value, 0.9×10^3 cm^{-1}, obtained from Hush analysis (eq 24) of the IT transition.[42b]

Conclusions

The role played by chemical bridges in ET processes between donor and acceptor is actually a very complex one. In fact, it is dependent not only on a variety of intrinsic structural and electronic features (chemical nature, length, redox properties) of the bridge, but also on the donor and acceptor units used, on their connection to the bridge, on whether the ET process is thermally or photochemically induced, in this latter case on whether it follows excitation of the donor (*oxidative* PET) or of the acceptor (*reductive* PET), and on whether the forward (CS) of backward (CR) process is considered. In this tutorial review we have tried to lay down in a simple, schematic fashion a general conceptual framework able to encompass the various aspects of this multifaceted problem. This framework makes use of the superexchange model, by which donor and acceptor undergo indirect electronic coupling mediated by ET or HT virtual states involving the bridge. Provision is also made, depending on the actual energies of such states, for a switch from superexchange to real electron (or hole) injection from the photoexcited unit into the bridge, thus approaching a "molecular wire" behavior.

From the vast literature on ET in D-B-A systems, specific examples have been chosen to illustrate single aspects of this complex problem. In particular: (i) the possibility to control ET rates by applying substituents or inserting specific molecular units in the bridge (Section 6.1); (ii) the relative rates of CS and CR in photoinduced ET, and the complex role played by the bridge in this respect (Section 6.2); (iii) the transition from superexchange to charge injection in photoinduced ET across

modular bridges of various length (Section 6.3); (iv) the question of how bridge-specific can the distance-dependence parameter β be considered (Section 6.4); (v) the ability of bridges to kinetically discriminate between reductive and oxidative excited state quenching and recombination processes (Section 6.5); (vi) how the same superexchange arguments used to discuss photoinduced ET in D-B-A systems can be applied in the context of intervalence transfer optical transitions of mixed-valence compounds (Section 6.6).

Acknowledgements

Financial support from the Italian MIUR (FIRB RBAP11C58Y "NanoSolar", PRIN 2010 "Hi-Phuture") and COST action CM1202 "PERSPECT-H_2O" is gratefully acknowledged.

Notes and references

[a] *Dipartimento di Scienze Chimiche e Farmacautiche, Università di Ferrara, and Centro Interuniversitario per la Conversione Chimica dell'Energia Solare (SOLARCHEM), sez. di Ferrara, Via Fossato di Mortara 17-19, 44121 Ferrara, Italy. E-mail: snf@unife.it*
[b] *Dipartimento di Scienze Chimiche,Università di Messina and Centro Interuniversitario per la Conversione Chimica dell'Energia Solare (SOLARCHEM), sezione di Messina, Via F. Stagno d'Alcontres 31, 98166 Messina, and ISOF-CNR, Via Gobetti 101, 40129 Bologna, Italy. E-mail: campagna@unime.it*

¶ This may not always be true, particularly with unsaturated bridges, where HOMO and LUMO energy levels may change with the length of the conjugated system. This may cause deviations from the expected exponential dependence of electronic coupling and ET rate constants, and in extreme cases abrupt changes in ET mechanisms. Some examples are discussed later on.

§ From eq 21, the β value depends not only on the type of bridge (through H_{mn}), but also on the donor-acceptor couple (through the energy difference ΔE). The energy of the ET virtual states refers to the intersection of reactant and product states and is thus expected to be different in the two series of dyads. The expectation that the dyads with the better acceptor DQ^{2+} should have somewhat larger ΔE values, and thus a slightly larger β, is qualitatively borne out. A more evident example of such ΔE effect is discussed in Section 6.4.

‡ With this type of spacers, given the donor and acceptor units used, the energies of the virtual states correlate with the reduction and oxidation potentials (related to the LUMO and HOMO energies) of the corresponding oligo-phenyls.[43] For n = 1-5: E_{red} = −3.35, −2.72, −2.44, −2.32, −2.24 (V vs SCE); E_{ox} = 2.40, 1.81, 1.56, 1.43, 1.36 (V vs SCE).

† In the CS processes of dyads **7(n)** and **8(n)**, assuming ca. 2.0 eV as the energy of the reactant/product state, the ΔE for the ET virtual states spans for n = 1-3 the range 2.0 ± 0.5 eV. In eq 21, this would yield changes in β of ± 15%.

A thorough discussion of the effects of length-dependent bridge energetics on the distance dependence of rate constants is given by Petterson, et al.[44]

‖ For CR of dyads **8(n)** with n = 1-3, assuming ca. 1.7 eV as the energy of the reactant/product state, ΔE values for the ET virtual states lie in the 2.94-2.03 eV range, whereas those for the HT states span the 1.22-0.38 eV range.

** In fact, for more extended dyads of the **8(n)** series (n = 4,5), the oligo-phenylene bridge becomes so easy to oxidize that a completely different quenching mechanism sets in (rather than oxidative quenching by the DQ^{2+} acceptor, reductive quenching by the bridge).[21]

1 V. Balzani, Ed. *Electron Transfer in Chemistry*; Wiley-VCH: Weinheim, Germany, 2001.
2 (a) Ref. 1, Vol 1, *Principles, Theories. Methods and Techniques*, part 1; (b)M. McGuire and G. McLendon, *J. Phys. Chem*., 1986, **90**, 2549; (c) K. V. Mikkelsen and M. A. Ratner, *Chem. Rev*., 1987, **87**, 113; (d) J. N. Onuchic and D. N. Beratan, *J. Phys. Chem*., 1988, **92**, 4817; (e) Ref. 1, Vol 1, *Principles, Theories. Methods and Techniques*, part 2.
3 Ref. 1, Vol. 3. *Biological and Artificial Supramolecular Systems*, part 1.
4 H. B. Gray and J. R. Winkler, *Biochim. Biophys. Acta*, 2010, **1797**, 1563.
5 Ref. 1, Vol 4. *Catalysis of Electron Transfer, Heterogeneous and Gas-phase Systems.*
6 M. Grätzel, *J. Photochem. Photobiol. C*, 2003, **4**, 145.
7 C. Brabec, V. Dyakonov, J. Parisi and N. S. Sariciftci, Ed., *Organic Photovoltaics*, Springer Verlag (Berlin, 2003).
8 (a) J. N. Onuchic and D. N. Beratan, *J. Am. Chem. Soc*., 1987, **109**, 6771; (b) K. V. Mikkelsen and M. A. Ratner, *J. Phys. Chem*., 1989, **93**, 1759; (c) M. D. Newton, *Chem. Rev.* 1991, **91**, 767. (d) M. R. Wasielewski, *Chem. Rev.*, 1992, **92**, 435. (e) K. D. Jordan and M. N. Paddon-Row, *Chem. Rev.* 1992, **92**, 395. (f) P. F. Barbara, T. J. Meyer and M. A. Ratner, *J. Phys. Chem.* 1996**, 100**, 13148. (g) D. Gust, T. A. Moore and A. L. Moore, *Acc. Chem. Res.*, 2001, **34**, 40. (h) S. Fukuzumi, *Bull. Chem. Soc. Jpn.* 2006, **79**, 177. (i) B. Albinsson and J. Mårtensson, *J. Photochem. Photobiol. C*, 2008, **9**, 138O. (j) S. Wenger, *Acc. Chem. Res.*, 2011, **44**, 25.
9 J. Jortner, M. Bixon, Eds. *Electron Transfer- From Isolated Molecules to Biomolecules*, Advances in Chemical Physics Series, Vol 106, Wiley, New York, 1999.
10 (a) N. R Kestner, J. Logan and J. Jortner, *J. Phys. Chem.*, 1974, **78**, 2148; (b) J. Jortner, *J. Chem. Phys.*, 1976, **64,** 4860; (c) J. Ulstrup and J. Jortner, *J. Chem. Phys.*, 1975, **63**, 4358.
11 (a) B. S. Brunschwig, J. Logan, M. D. Newton, and N. Sutin, *J.Am. Chem. Soc*., 1980, **102**, 5798 (b) P. Siders and R. A. Marcus, *J. Am. Chem. Soc.*, 1981, **103**, 741; (c) N. Sutin, *Prog. Inorg. Chem*., 1983, **30**, 441; (d) R. A. Marcus and N. Sutin, *Biochim. Biophys. Acta*, 1985, **811**, 265.
12 J. R. Miller, J. V. Beitz and R. K. Huddleston, *J. Am. Chem. Soc*., 1984, **106**, 5057.
13 T. J. Meyer and H. Taube, *Comprehensive Coordination Chemistry*, Pergamon, Oxford, 1987, Vol. 1, p. 331.
14 (a) J. Halpern and L. E. Orgel, *Discuss. Faraday Soc*., 1960, **29**, 32; (b) H. M. McConnell, *J. Chem. Phys.*, 1961, **35**, 508; (c) B. Mayoh and P. Day, *J. Chem. Soc., Dalton Trans*., 1974, 846; (d) J. R. Miller and J. V. Beitz, *J. Chem. Phys.*, 1981, **74**, 6746; (e) D. E. Richardson and H. Taube, *J. Am. Chem. Soc.*, 1983, **105**, 40.
15 (a) D. Segal, A. Nitzan, W. B. Davis, M. R. Wasielewski and M. A. Ratner, *J. Phys. Chem. B*, 2000, **104**, 3817; (b)M. N. Paddon-Row, In *Electron Transfer in Chemistry*; V. Balzani, Ed.; Wiley-VCH: Weinheim, Germany, 2001; Vol. III, Chapter 2.1, p 179; (c) F.

Scandola, C. Chiorboli, M. T. Indelli and M. A. Rampi, In *Electron Transfer in Chemistry*; V. Balzani, Ed.; Wiley-VCH: Weinheim, Germany, 2001; Vol. III, Chapter 2.3, p 337; (d) K. Petersson, J. Wiberg, T. Ljungdahl, J. Mårtensson and B. Albinsson, *J. Phys. Chem. A*, 2006, **110**, 319; (e) A. Arrigo, A. Santoro, M. T. Indelli, M. Natali, F. Scandola and S. Campagna, *Phys. Chem. Chem. Phys.*, 2014, **16**, 818.

16 J. Jortner, M. Bixon, T. Langenbacher and M. E. Michel-Beyerle, *Proc. Natl. Acad. Sci. USA*, 1998, **95**, 12759.

17 M. R. Wasielewski, M. P. Niemczyk, D. G. Johnson, W. A. Svec and D. W. Minsek, *Tetrahedron*, 1989, **45**, 4785.

18 J. Wiberg, L. Guo, K. Patterson, D. Nilsson, T. Ljungdahl, J. Mårtensson and B. Albinsson, *J. Am. Chem. Soc.*, 2007, **129**, 155.

19 D. Hanss, M. E. Walther and O. S. Wenger, *Coord. Chem. Rev.*, 2010, **254**, 2584, and references therein.

20 M. T. Indelli, C. Chiorboli, L. Flamigni, L. De Cola and F. Scandola, *Inorg. Chem*., 2007, **46**, 5630.

21 M. Indelli, M. Orlandi, C. Chiorboli, M. Ravaglia, F. Scandola, F. Lafolet, S. Welter and L. De Cola, *J. Phys. Chem. A*, 2012, **116**, 119.

22 M. M. Toutounji and M. A. Ratner, *J. Phys. Chem. A*, 2000, **104**, 8566.

23 A. C. Benniston, A. Harriman, P. Li, C. A. Sams and M. D. Ward, *J. Am. Chem. Soc*., 2004, **126**, 13630.

24 M. T. Indelli, C. A. Bignozzi, A. Harriman, J. R. Schoonover and F. Scandola, *J. Am. Chem. Soc.*, 1994, **116**, 3768.

25 J. Fortage, F. Puntoriero, F. Tuyèras, G. Dupeyre, A. Arrigo, I. Ciofini, P. P. Lainé and S. Campagna, *Inorg. Chem.*, 2012, **51**, 5342.

26 J. Fortage, G. Dupeyre, F. Tuyèras, V. Marvaud, P. Ochsenbein, I. Ciofini, M. Hromadová, L. Pospísil, A. Arrigo, E. Trovato, F. Puntoriero, P. P. Lainé and S. Campagna, *Inorg. Chem*., 2013, **52**, 11944.

27 E. A. Weiss, M. J. Ahrens, L. E. Sinks, A. V. Gusev, M. A. Ratner and M. R. Wasielewski, *J. Am. Chem. Soc.*, 2004, **126**, 5577.

28 W. B. Davis, W. A. Svec, M. A. Ratner and M. R. Wasielewski, *Nature*, 1998, **396**, 60.

29 D. Hanss and O. S. Wenger, *Inorg. Chem.*, 2008, **47**, 9081.

30 D. Hanss and O. S. Wenger, *Inorg. Chem.*, 2009, **48**, 671.

31 M. Natali, M. Ravaglia, F. Scandola, J. Boixel, Y. Pellegrin, E. Blart and F. Odobel, *J. Phys. Chem. C*, 2013, **117**, 19334.

32 M. T. Colvin, A. B. Ricks and M. R. Wasielewski, *J. Phys. Chem. A*, 2012, **116**, 2184, and references therein.

33 (a) D. E. Richardson and H. Taube, *J. Am. Chem. Soc.*, 1983, **105**, 40; (b) C. Creutz, *Prog. Inorg. Chem.*, 1983, **30**, 1. (c) B. S. Brunschwig, C. Creutz and N. Sutin, *Chem. Soc. Rev.*, 2002, **31**, 168. (d) K. D. Demadis, C. M. Hartshorn and T. J. Meyer, *Chem. Rev.*, 2001, **101**, 2655.

34 (a) J.-P. Launay, *Chem. Soc. Rev.*, 2001, **30**, 386; (b) C. Lambert, G. Nöll and J. Schelter, *Nat. Mater.*, 2002, **1**, 69. (c) O. Wenger, *Inorg. Chim. Acta*, 2011, **374**, 3; (d) A. Heckmann and C. Lambert, *Angew. Chem., Int. Ed.*, 2012, **51**, 326.

35 (a) S. Campagna and G. Giuffrida, *Coord. Chem. Rev*., 1994, **135-136**, 517; (b)D. M. D'Alessandro and F. R. Keene, *Chem. Soc. Rev.*, 2006, **35**, 424.

36 N. S. Hush, *Prog. Inorg. Chem.*, 1967, **8**, 391.

37 A.-C. Ribou, J.-P. Launay, K. Takahashi, T. Nihira, S. Tarutani and C. W. Spangler, *Inorg. Chem.*, 1994, **33**, 1325

38 C. Lambert and G. Nöll, *J. Am. Chem. Soc.*, 1999, **121**, 8434.

39 M. J. Powers and T. J. Meyer, *J. Am. Chem. Soc.*, 1978, **100**, 4393.

40 G. M. Tom, C. Creutz and H. Taube, *J. Am. Chem. Soc.*, 1974, **96**, 7827.

41 A. C. Benniston, A. Harriman, P. Li, C. A. Sams and M. D. Ward, *J. Am. Chem. Soc.*, 2004, **126**, 13630.

42 (a) C. Creutz, M. D. Newton and N. Sutin, *J. Photochem. Photobiol. A: Chem.*, 1994, **82**, 47; (b) B. S. Brunschwig, C. Creutz and N. Sutin, *Coord. Chem. Rev*., 1998, **177**, 61; (c) C. E. B. Evans, M. L. Naklicki, A. R. Rezvani, C. A. White, V. V. Kondratiev and R. J. Crutchley, *J. Am. Chem. Soc.*, 1998, **120**, 13096.

43 K. Meerholz and J. Heinze, *Electrochimica Acta*, 1996, **41**, 1839.

44 K. Pettersson, J. Wiberg, T. Ljungdahl, J. Mårtensson and B. Albinsson, *J. Phys. Chem. A*, 2006**, 110**, 319.

KEY LEARNING POINTS

for the tutorial review:

Photoinduced electron transfer across molecular bridges. Electron- and hole-transfer superexchange pathways by Mirco Natali, Sebastiano Campagna and Franco Scandola, are as follows:

-photoinduced electron transfer

-superexchange theory

-virtual states involving bridge orbitals

-charge recombination

-modular bridges

Photos and biographies for the *Chemical Society Reviews* invited article: **Photoinduced electron transfer across molecular spacers. Electron- and hole-transfer superexchange pathways**.

 **Mirco Natali**	Mirco Natali received his master degree in Chemistry cum laude from the University of Ferrara in 2010, working on porphyrin-cobaloxime dyads for photoinduced hydrogen production. In 2011 he joined Prof. Scandola's group at the University of Ferrara as a Ph.D. student. His research is focused on the field of artificial photosynthesis, in particular on the study of charge separation systems and photoinduced water splitting.
 **Sebastiano Campagna**	Sebastiano Campagna received his Laurea in Chemistry from the University of Messina in 1983. After over 10 years spent in the research group of Prof. Vincenzo Balzani at the University of Bologna, he covers a professorship position at the University of Messina since 1998. His research interests are in the field of supramolecular photochemistry, with particular emphasis on artificial photosynthesis.
 **Franco Scandola**	Franco Scandola is Emeritus at the Department of Chemistry of the University of Ferrara, where he has been Professor of Inorganic Chemistry since 1980. His main interests lie within the field of supramolecular photochemistry. Current research includes fundamental aspects of energy and electron transfer, photophysics of self-assembling multichromophoric systems, design of functional units of artificial photosynthesis.

A tutorial review outlining a general conceptual framework, based on superexchange, to discuss the role of chemical bridges in photoinduced electron transfer processes.